

1

# 1 STRAW tubes

The option for STRAW tubes is similar as in NA62 experiment with one main difference – the length is twice longer(  $5m$  versus  $2.1m$ ).  
The next table. 1 describe STRAW tube options.

Parameter name	Value
wire	$30\mu m$ gold-plated Tungsten
straw length	$5m$
Voltage	$1750V$
inner tube radius	$9.8\ mm$
wire medium density	$19.3\ g/cm^3$
Wire tension	$\sim 90\ g$
Working tube gas mixture	$Ar70\%\ CO_230\%$

Табл. 1: STRAW tube parameters

## 2 Signal

Computer program Garfield [1] is designed for detailed simulation of two- and three-dimensional drift chambers. So we will perform STRAW tube studies using this program.

Charged particle create elector-ion pairs wile traverse the drift tube. Electrons under affecting the electric field drift to the wire anode 1. During the travel they increase their energy and invoke avalanche. Therefore they produce a measurable signal.

Initial electrons drift to the wire due to the electrical field between the wire and the tube wall. Electrons ionize gas molecules due to the high electric field around the wire, especially near the wire when the electric becomes very strong. Subsequently readout electronics process the signal induced on the wire.

The event registers if signal reach some a threshold voltage (Fig. 2). So the value of threshold is a key factor on the way of searching optimal setting for signal processing procedure.

We have to set threshold as low as possible but enough far from noise to achieve highest value of relation true/false detected track and tube efficiency.

A variation of the signal height introduces a variation in the time when the signal passes the threshold and is considered to be the main contribution to the STRAW tracker resolution.

In the track reconstruction software(GARFIELD [1] an effective TR-relation is used. It only describes the relation between the drift time and the distance from the track to the wire, which differs from the distance to the ionization cluster. The shape of the TR-relation is defined by the drift velocity of the ionization cluster inside the straw. The electric field increases towards the wire,

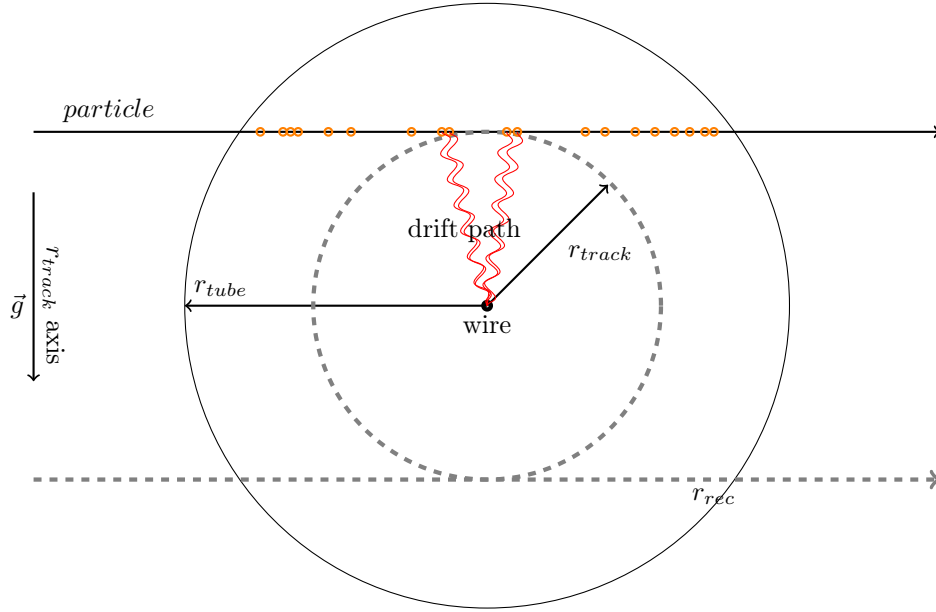


FIG. 1: Schematic view of a particle passing the straw and producing ionization clusters. The ionization cluster electrons drift to the wire and induce the signal. Only the earliest signal is detected. The closest distance from the track to the wire,  $r_{track}$ , and radius of the straw,  $r_{tube} = 2.45mm$ , are also indicated.

37 leading to a non linear TR-relation. Currently almost parabolic dependence is  
 38 used, and easily can be fitted by function (10).

39 The drift time versus the unbiased distance distribution and the result of the  
 40 fit are shown in Fig. 12a. Noise hits under the main distribution, i.e. at earlier  
 41 times, are due to primary or secondary particles ( $\delta$ -rays) passing the straw at a  
 42 closer distance to the wire, consequently producing an earlier signal.

43 Muon  $\mu$  was chosen as test particle for simulation with energy  $1GeV$ . You  
 44 can see some of typical tracks from the  $\mu$  through the tube Fig.7a,7b. Initial  
 45 clusters along the track are marked by orange points on the figure.

## 46 2.1 Leakage noise

47 Every time we deal with different kind of noise. Basically it is noise from leakage  
 48 current through readout electronics.

49 As will be discussed further we analyse not the current invoked by particle  
 50 but the output voltage from amplifier. In GARFIELD we able convolute input  
 51 current  $I(t)$  with electronic response function (1):

$$f_{resp} = A \cdot (e^{-t/0.005} - e^{-t/0.030}) \quad (1)$$

52 Noise is very important for every calculations and it makes bit impact on

53 straw precision and straw efficiency. So we can't rely on results until we receive  
 54 signal and noise from real STRAW tube prototypes.

55 Convolution smooth input current. Experiments that used to drift tubes  
 56 (such as ??(advise of Iouri Guz)) say that the noise should have gauss distri-  
 57 bution with RMS equal to a amplitude of signal from 2000 electron in the tube -  
 58 electric noise charge (ENC). (This part should be clarified more precisely. Would  
 59 be good to include some results from noise measurements from STRAW tube  
 60 samples. In fig.2 you can see deposition from noise marked by blue line.

61 On the figure fig.2 The time stamp  $Time = 0$  correspond to the time muon  
 62 cross tube. The convolution function smooths and spreads input current. It  
 63 mean that the output voltage in GARFIELD does not contain part of signal  
 64 before hit event time stamp.

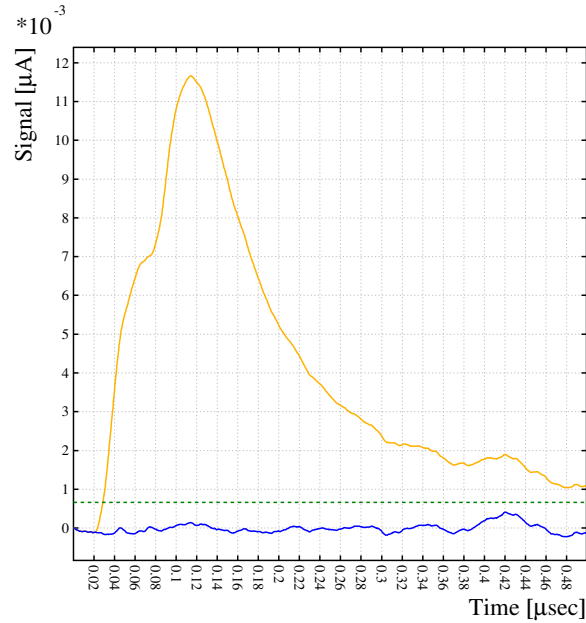


FIG. 2: Example of output signal  $V(t)$  after convolution(front-end electronics) from central track(yellow line). The noise component of the same signal depicted by separate blue line. Green dashed line is a threshold for triggering drift time and equal to  $5\sigma$  of noise distribution.

## 65 2.2 STRAW efficiency

66 The interaction of charge particle with gas molecules have probabilistic nature.  
 67 For short distance tracks(somewhere at the tube periphery) the probability of  
 68 tracks that do not produce any electron/ion pair becomes significantly high.

69 The number of produced ionization clusters directly affects the hit efficiency profile. [2] Smaller ionization length increase hit efficiency because of more  
70 ionization clusters per length unit are producing. In GARFIELD we can easily  
71 calculate amount of clusters per track. In fig. 4b you can see a distribution of  
72 number of clusters per central track for our STRAW tube. It mean that straw  
73 efficiency will be lower at the tube wall( see fig. ??).  
74

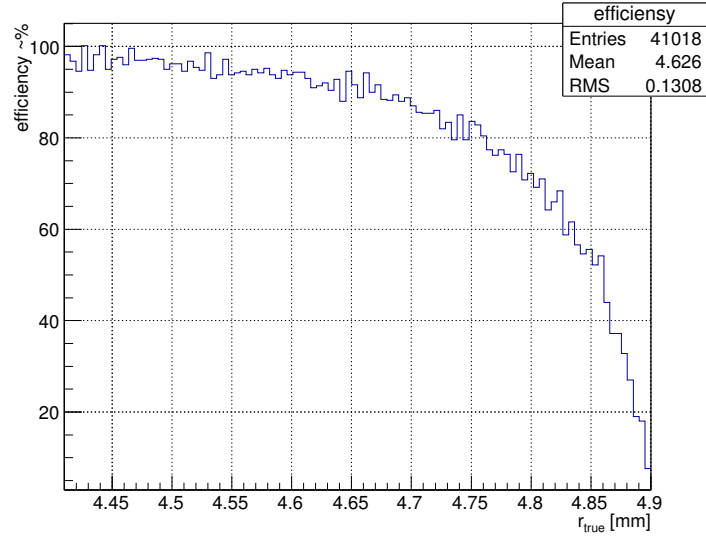
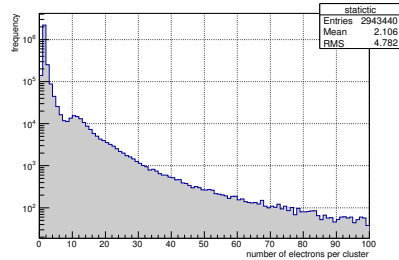
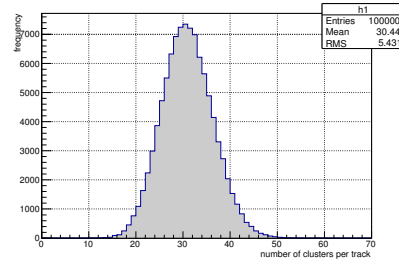


FIG. 3: Straw tube efficiency. Result of homogeneous penetrating periphery of tube by 50k events(scaled down by factor of 5.  $\frac{50k \text{ events}}{100bin} = 500 \frac{eventst}{bin}$ ).



(a) electrons per cluster



(b) number of clusters per central track

FIG. 4: There are big amount of graphs. So I'm trying to pair it. ere we can write something if needed. Some common description of (a) and (b) figures?

75 From the figure ?? we can conclude that the efficiency of tube is 100% almost  
76 in whole region covered by tube except pre wall region which is quite small.

77 Increasing the gas mixture density or increasing the tube radius for the same  
78 gas density can increase tube efficiency. Have to check this in feature studies.

### 79 3 Gain

80 If multiplication occurs, the increase of the number of electrons per path  $ds$  is  
81 given by

$$dN = N\alpha ds \quad (2)$$

82 The coefficient  $\alpha$  is determined by the excitation and ionization cross sections  
83 of the electrons that have acquired sufficient energy in the field. It also depends  
84 on the various transfer mechanism and electric field  $E$  and increases with the  
85 field because the ionization cross-section goes up from threshold as the collision  
86 energy  $\varepsilon$  increases. As we can suppose the coefficient  $\alpha$  is of big amount of  
87 parameters.

88 The amplification factor  $G$  on a wire(that is more interesting for us) is given  
89 by integrating (2) between the point  $s_{min}$  where the field is just sufficient to  
90 start the avalanche and the wire radius  $a$ :

$$G = N/N_0 = \exp \int_{s_{min}}^a \alpha(s) ds \quad (3)$$

91 GARFIELD can provide us by amplification factor  $G$  for any point of the  
92 tube(because  $G$  is coordinate dependent magnitude). The amplification factor  
93 is equal almost in whole tube space except neighbourhood near the wire because  
94 electric field becomes significantly high only near the wire (see figs 5a, 5b). When  
95 the wire is shifted from the center of the cube the electric field in area close to  
96 the wire is the same as in centered state. So the amplification factor  $G$  is quite  
97 similar in both cases.

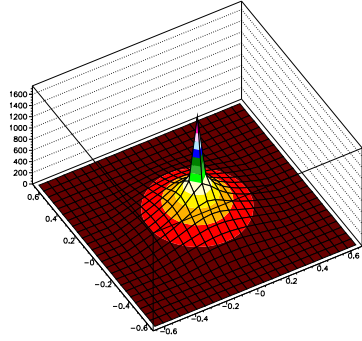
98 Implementation of gain value calculation is not so reliable in GARFIELD(especially  
99 fortran version). So we can reach better results using Garfield++ (which is newer  
100 and take into consideration more effects).

101 On the Fig. ?? you can see that the gain  $G(V)$  have precisely exponential  
102 dependence. This is frankly does not inspire confidence. The difference can be  
103 up to 100% (us Rob Veenhof[1] said).

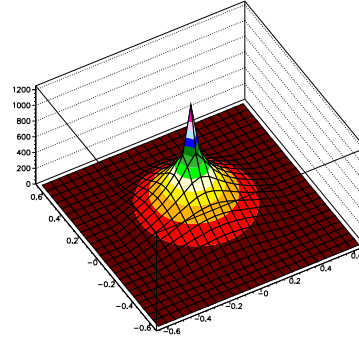
### 104 4 Wire sagging

105 Easy to predict that the shifting of the wire invoke distorting an electric field(see  
106 figs 5a,5b) and drift path for electrons/ions inside the tube(see fig.7a and fig.7b).  
107 The rt-relation for track reconstruction directly depend on the wire position in  
108 the tube. So rt-relation lose it's previous symmetry(see next sections).

109 The direction of sagging is unpredictable when the wire is centered and the  
110 straw has vertical orientation. Impact of gravitation field into the wire does not



(a) electric field for centered wire



(b) electric field for 1mm shifted wire

FIG. 5: Electric field intensity map for different wire position in the cube calculated in GARFIELD software. Conditions for those plots are described in table 1

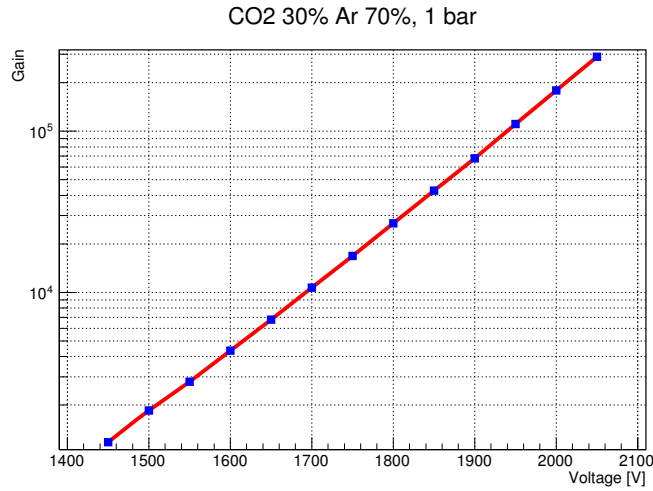


FIG. 6: Dependence of the gain of the voltage applied to the wire. The rest of STRAW tube settings you can find in table 1. need add gain(v) graph for shift wire STRAW tube for comparison

111 make any effect in this state. But we can avoid this ambiguity by setting straws  
 112 horizontally. This condition is necessary to make track reconstruction possible.  
 113 We estimate significant wire sagging (by comparison to the tube radius)  
 114 because of wire attracts to the tube under affecting of gravitation and electric  
 115 field force.

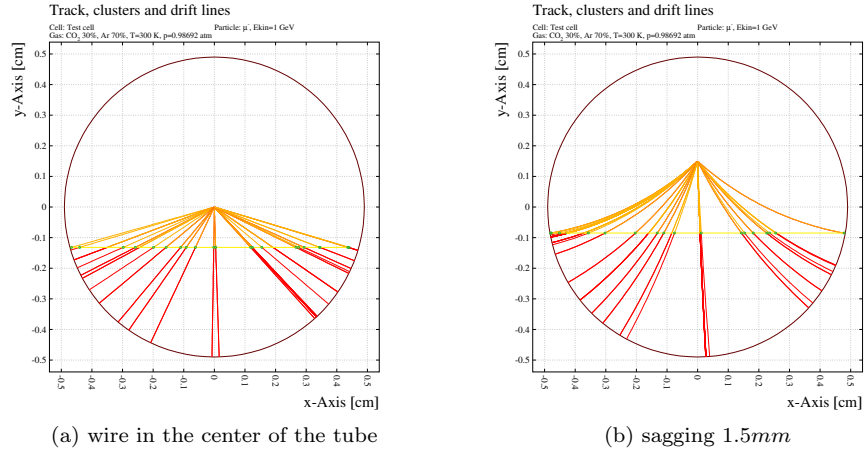


FIG. 7: An example of tracks from the on the tube for different position of the wire from GARFIELD simulations. Initial clusters marker by green. Drift lines for electrons marked by yellow, ions – red lines.

116 You can see a profile of wire sagging of 5m length wire in 1cm diameter  
117 straw tube and 1750V voltage on the fig.8 calculated in GARFIELD  
118 [1].

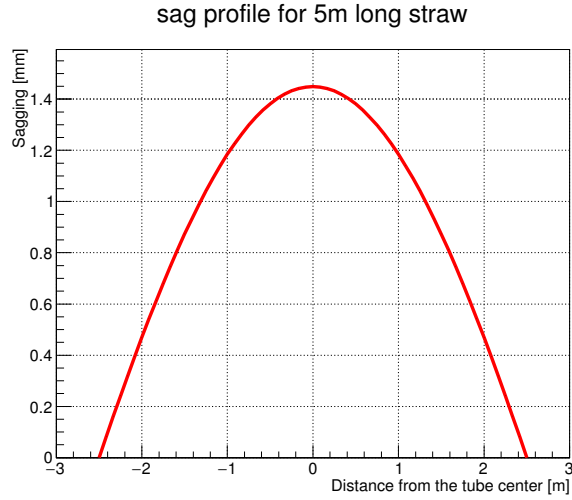


FIG. 8: Wire sag profile under electric and gravitation field calculated in GARFIELD. All options for this straw system are described in table 1.

119 The calibration of STRAW tube with sagged wire is more difficult by compari-  
120 son to the mode without sagging.



121 Variation of wire tension, wire radius should be taken into account as high  
122 affect factor for sag value.

## 123 5 Sag estimation

124 In this section we have to find out method for assessing sagging. This is key  
125 step that makes track reconstruction procedure possible.

126 At first we have to think on data we can use for such kind of calculations.  
127 Much attractable information we can extract from drift time distribution.

128 The wire sags under electric and gravitation force. Therefore the sag value  
129 is differ along the tube(fig 8). But we can separate collected data for different  
130 position along the tube. STRAW tube detector consist of several parallel layers  
131 of tubes at some angle to each other. So we can easily fix longitudinal position for  
132 tracks that cross several crossed tubes(at least two). Collimation is also possible  
133 via scintillator triggering before and after STRAW tube.

134 Lets say we can install our STRAW tube into homogeneous particle flow and  
135 save drift time distribution for some narrow section of the tube. These distri-  
136 butions are different from each other(see example on Figure ??). The difference  
137 between diagrams increasing with sag difference. So it is good possibility for sag  
138 calibration.

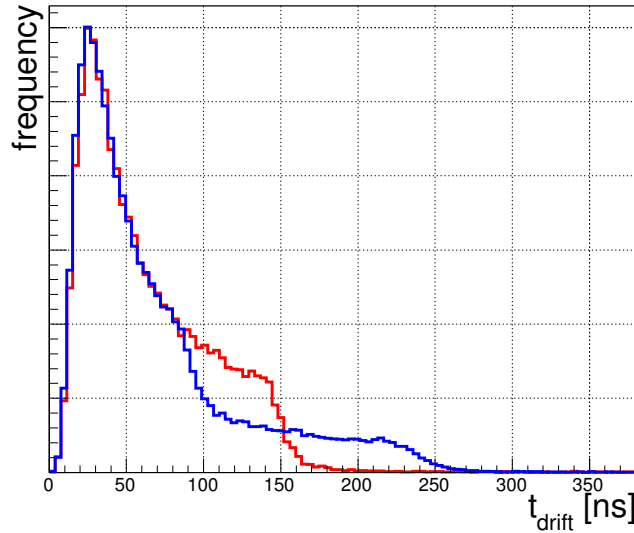


FIG. 9: Drift time distribution for a homogeneous irradiation with a centered wire (red) and for a wire offset of 0.9 mm (blue).

139 Then we have to bind each drift time distribution with appropriate sag value.  
140 This is part of laboratory work when sag profile measurements can be performed

141 via optical method prior to the exposition.

142 Distributions on graph ?? contain GARFIELD simulations for some certain  
 143 wire(not for section of sagged wire)because of GARFIELD can handle only two-  
 144 dimensional tasks.

145 Lets say we have an equipment for scanning the tube to measure wire saggi-  
 146 ng profile. After profile measurements we divide our tube into sections. Wire  
 147 position within separate section should be within desired precision.

148 So we need divide our tube into 57 sections (see figure 10) if maximum of  
 149 wire offset(at the center of the tube) is equal to  $1.45mm$  and desired precision  
 150 is  $50\mu m$ .

$$N_{halftube} = \frac{1.45mm}{50\mu m} = 29; \quad (4)$$

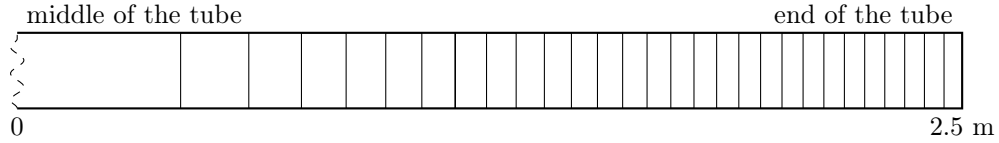


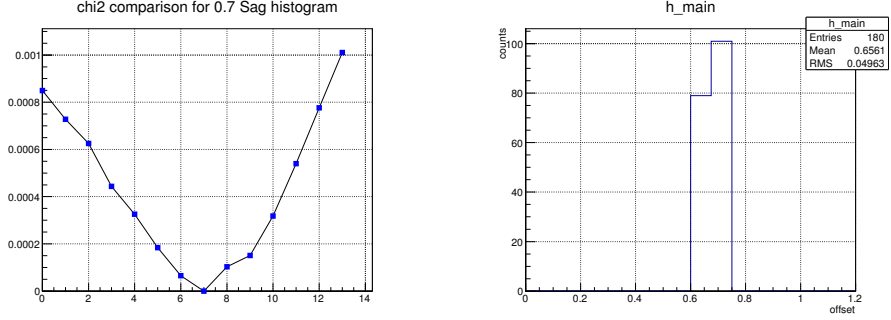
Рис. 10: Tube sectioning. Sag value at the tube center is  $1.45mm$ . Difference of wire sag value from section to section is  $50\mu m$

151 Then we need an exposition of sufficient number of events for every of secti-  
 152 ons(at least 50k events). There can be troubles time of exposition time because  
 153 square of sections at the end of the tube is quite small. So the time of exposition  
 154 of distant sections will be inversely much longer.

155 The next step is to find dependence of dt-distribution shape with wire offset.  
 156 The point that we can evaluate matching between histograms via  $\chi^2$  criteria.  
 157 As we can see in the figure 11a the comparison of  $\chi^2$  has smooth dependence  
 158 across increasing of wire offset for high statistic histograms.

159 So the preliminary algorithm for sag estimation is:

- 160 1. measure wire sag profile via optical method;
- 161 2. make a sectioning for wire sag profile;
- 162 3. collect enough amount of events for every of dt-distribution and save this  
 163 core distribution into lookup table.
- 164 4. measure dt-distribution for new drift tube section that is subject of study.
- 165 5. calculate  $\chi^2$  criteria for this current dt-distribution with each of core di-  
 166 stribution. The minimum from set of  $\chi^2$  estimations mean best match  
 167 between histograms and consequently closest wire sag value that match  
 168 to this core histogram (see fig 11a).



(a) Series of  $\chi^2$  of comparison 0.7mm sag core td-distribution with each each of core histograms. 14 core histograms for sag diapason 0...1.3mm with step of 100 $\mu$ m

(b) Distribution of wire offset reconstruction from 180 series 5k events each. 50k events for *core* template histograms. True bias is 0.063mm. 1 bin = 0.1 mm.

Рис. 11: Wire position(offset) reconstruction

On the figure 11b you can see distribution wire sag calculation for 180 histograms with 5k events statistic. Precision in this case  $\sim 50\mu$ . The algorithm of sag estimation is pretty simple: wire offset value equal to the as best match between *test* and *core* histogram.

After we know sag value at some points of the tube or every where we can make one awesome collective analysis. The smoothing of wire offset value along the tube will give us much more precision results. Fitting of sag value at every point of  $s(l)$  by some parabolic function should provide us the best results.

Here i would like to put total plot of wire sag profile and compare reconstructed profile with true profile.

## 6 Track reconstruction

The time between the track hit time stamp and the signal rising edge is a measure for *drift time* of these electrons. The relation between the *drift time* and the distance from the track to the center of the tube(wire while no sag for centered wire) is called *drift time - distance relation* or *rt-relation*.

The drift time  $t$  is a function of track position relative to the wire(so it's means the track position) and electric field along the drift trajectory.

Assumed that the working position for straws will be parallel to the particle bunch, and acceptance of particle spreading will not be significantly big. So tracks will be collinear each other within every separate unit STRAW tube.

Summing the above mentioned we have one dimension task – reconstruct tracks on vertical axis<sup>1</sup> (see example outcome rt-distribution  $t = t(r, s = 0)$  in Fig.12a ) even the wire sagging. Sagging will be always down thanks to gravitation force  $\vec{g}$ .

<sup>1</sup>An example of single track reconstruction which explains the approximate procedure of

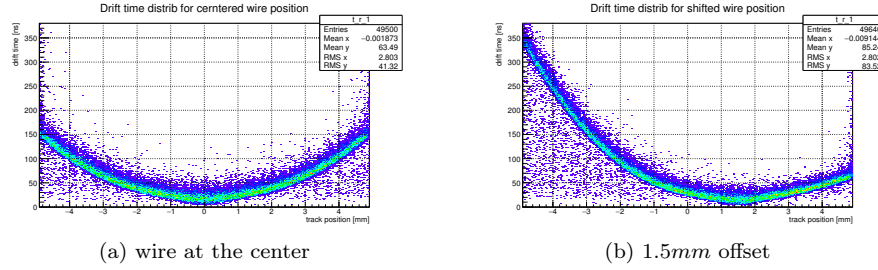


Рис. 12: Distribution of drift time  $t_{drift}$  as function of track position  $r_{track}$  relatively to the tube center

203 The rt-relation is differ along the tube because different wire position  $s$ . Thus  
 204 we have for the drift time

$$t_{drift} = t_{drift}(r_{track}, s) \quad (5)$$

205 The idea to STRAW tube is to find the inverse dependence

$$r_{track} = r_{track}(t_{drift}, s) \quad (6)$$

206 From the section "Sag estimation" we can find sag profile for straw. Therefore  
 207 the rt-calibration becomes 1 dimension less:

$$r = r(t, s = const) \quad (7)$$

## 208 6.1 How drift time resolution depend on wire offset?

209 Distorting of electric field inside the tube invoked by wire displacement from the  
 200 center position will make an effect on drift time. Here we are going to estimate  
 201 magnitude of drift time change.

202 As was noted above we make a binning for our data along the  $r_{track}$  (fig. 12a,  
 203 12b). The resolution at every bin is RMS of every bit digram (fig.??).

204 We are dealing with probabilistic nature of clustering that spread rt-relation  
 205 from thin line. The leakage noise is also present in calculation but the effect of  
 206 it is not very high (especially in this calculation).

207 Every plot of output current (see fig. 2) consist of 1000 equidistant frames.  
 208 The threshold is set to  $5\sigma$  of noise. Leakage noise make effect on drift time  
 209 measurements in case its amplitude becomes higher than threshold value in  
 210 range from  $t = 0$  to  $t = t_{drift}$ . At five-sigma there is only one chance in nearly  
 211 two million that a random fluctuation would yield the result. The drift time for  
 212 tracks close to the tube edge can be up to  $150ns$  and  $300ns$  in case wire displaced.  
 213 The probability to meet noise above threshold value is less than 0.02%.

214 Another source of noise points on tr-distribution comes from  $\delta$ -electrons that  
 215 cause secondary ionisation in tube volume. The impact do only those electrons  
 216 which are emitted in the direction of the wire (see example on fig.14a).

reconstruction you can see on Fig.1

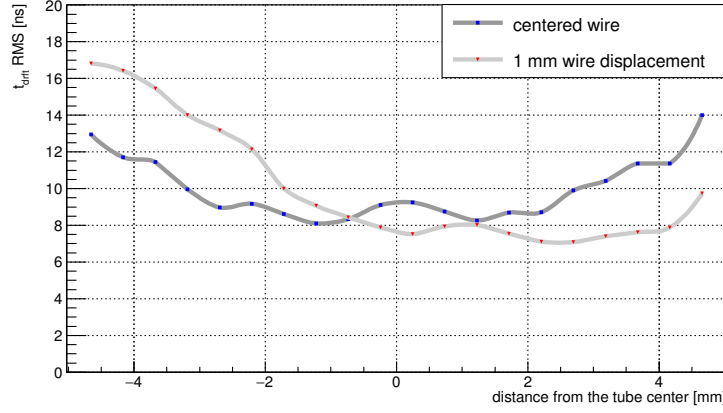


Рис. 13: Resolution of drift time as a function of distance from the wire.

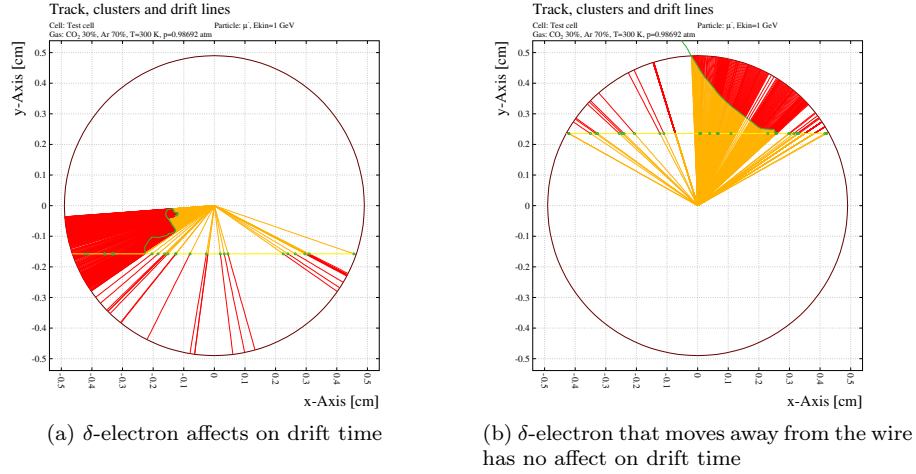


Рис. 14: Garfield simulation with  $\delta$ -electron presence. Red lines - ion trajectory, yellow - electrons. Trajectory of  $\delta$ -electron marked by green curve line.

217 The number of events out of TR-ralation because of  $\delta$ -electrons is quite small.  
 218 Especially percentage of events where  $\delta$ -electrons make effect on drift time is  
 219 less that 1% of total number of events in GARFIELD simulations.

220 Tube wall is very thin but particle still can cause  $\delta$ -electrons when crossing  
 221 it. GEANT4 studies show that such kind effect also presents in interaction of  
 222 muon with tube volume, and percentage of events with  $\delta$ -electron that affect  
 223 drift time even less that 0.2%.

## 224 6.2 Finding of rt-relation

225 The rt-relation depict relation between drift time and track position. So we can  
 226 easily find this law. The idea is to find the best fit of give data to achieve higher  
 227 resolution and avoid systematic errors.

228 The problem that we have to minimize influence of noise while fit. One  
 229 suppose that the noise have approximately homogeneous distribution of points  
 230 that locates below the main line of distribution. Consequently we can filter it  
 231 by fitting only points from regions with local point density higher that some  
 232 threshold value. Another way is to make a binning our distribution along the  
 233 track position and fit every 1-D histogram by Gaussian. Nevertheless our data  
 234 contain very small amount of "non-track"points.

235 Lets suppose we can fit every of tr-diagram by pair of analytic fit function  
 236 (8):

$$t(r_{track}) = e^{a_0 + a_1 r_{track}} \quad (8)$$

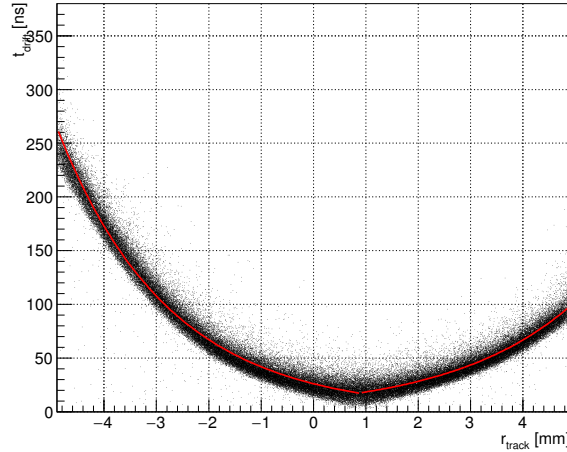


Рис. 15: TR-relation fitting for 0.9mm wire offset value

237 If the figure ?? you can see tr-relation. Fitting is not perfect because of using  
 238 simple fit function template (8). But we will use reverse to the (8) relation,  
 239 because we have to find  $r_{track}$  from known  $t_{drift}$ . We can do it be because the  
 240 aim of this studies is not a precision calibration but global evaluation affect of  
 241 wire sagging into total result.

242 As you can see in the figure ?? red fit line does not cover whole drift time  
 243 spectre. So events with drift time less than covered range (less than  $\sim 20ns$ )  
 244 counts as track through the wire:

$$r_{track}(t_{drift} < t_{min}) = r_{wire\ pos} \quad (9)$$

245 where  $t_{min} = \min(t_{drift}(r_{track}))$ ,  $r_{track} = \overline{(-r_{tube}, r_{tube})}$ . Respectively tracks  
 246 with drift time higher than maximum of fit function range artificially counts as  
 247 tracks with near tangents to the tube position  $r_{track} = \pm r_{tube}$  (because efficiency  
 248 decreases near the tube wall down to 20%).

### 249 6.3 How precision of track reconstruction depend on wire 250 position(wire displacement)

### 251 6.4 Джерела похибок

- 252 • Природна складова похибки визвана розподілом кластерів іонізованих  
 253 атомів вздовж треку МР-частинки.
- 254 • Похибка пов'язана безпосередньо з дрейфом електронів та йонів в труб-  
 255 ці. Залежить від параметрів електричного поля та складової газу в  
 256 трубці.
- 257 • Похибка пов'язана з ефектами поширення заряду від електромагнітної  
 258 лавини в дроті.
- 259 • Фактори електроніки – функція відгуку електроніки.

260 Instead of using the average value of the drift time residuals, a fit to the  
 261 distribution of unbiased drift time residuals is performed in a narrow range  
 262 around the peak. This allows to reduce the contribution of incorrectly assigned  
 263 hits

264 Для ясності опишемо дану процедуру поетапно

- 265 1. Оскільки TR розподіл симетричний відносно  $r_{track} = 0$  Рис. 12а, то  
 266 для підвищення статистики будемо аналізувати їх "суму".
- 267 2. з TR розподілу рис.12а будемо структурну діаграму шляхом розбит-  
 268 ття даних на секції вздовж  $r_{track}$  (ось X) і знаходимо середнє для таких  
 269 вибірок.
- 270 3. як видно з рис.12а в симуляціях є досить багато шуму - точки поза  
 271 головним "стержнем"розподілу. Тому для більш точних результатів  
 272 в побудові RT залежності цього шуму слід позбавитися. Як варіант  
 273 пропонуємо наступний критерій: вважати шумами всі точки, які зна-  
 274 ходяться на відстані більше  $2\sigma$  від середнього вибірки для кожної із  
 275 секцій від першої ітерації.
- 276 4. для "відфільтрованих"даних повторюємо пункт №2;
- 277 5. Апроксимуємо точки середнього з вибірок функцією (10)

$$y = e^{a_0 + a_1 x} \quad (10)$$

- 278 6. Знаходимо RT відношення як оберенену до (10) функцію. Результат  
 279 зображено червоною лінією на рис. 16

280 В даному випадку калібровочною кривою буде однозначна відповідність  
 281 між часом дрейфу і радіусом дотичного кола.

282 Для знаходження кривої  $r(t)$  складемо дві гілки розподілу Рис. 12а (пра-  
 283 воруч і ліворуч нуля), інвертуємо розподіл  $t_{drift}(r_{track}) \rightarrow r_{track}(t_{drift})$  і  
 284 виконаємо підгонку розподілу функцією виду (11).

$$r(t) = a_1 \log(t) + a_2 \quad (11)$$

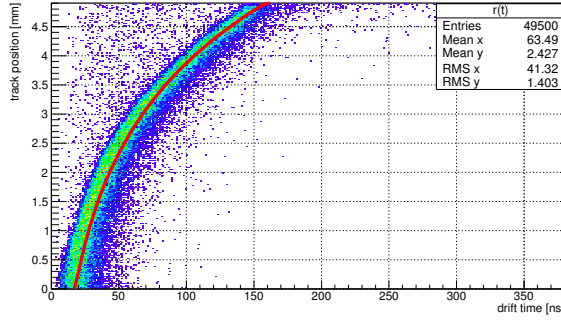


Рис. 16: RT-ralation(calibration line, figured in red color) between drift time  $t_{drift}$  and distance from the track  $r_{track}$ . The fit is performed in the range of  $0 < t_{drift} < 150ns$  and  $|r| < 4.9mm$

285 Далі наводимо параметри калібровочної кривої як результат фітування  
 286 розподілу  $t_{drift}(r)$  Рис. 16

287 •  $a_1 = 2.231 \pm 0.008$

288 •  $a_2 = 0.448 \pm 0.002$

#### 289 6.4.1 Precision of track reconstruction

#### 290 6.4.2 How precision of track reconstruction depend on wire di- 291 splacement

292 Для початку задамося питанням "як точність реконструкції треків зале-  
 293 жить від положення дроту (точніше від його відхилення від центрального  
 294 положення).

295 Відомо, що робочі зразки дрейфових трубок будуть працювати в гори-  
 296 зонтальному положенні. Зважаючи, що під дією гравітаційного поля дріт в  
 297 трубці буде прогинатися вниз, можна з певною достовірністю стверджувати  
 298 про подальше положення дроту, вже після підведення напруги в трубці.

299 Так виконаємо оцінку залежності точності вимірювання координати в  
 300 трубці по зміні часового розподілу.



### 6.4.3 Evaluation of track reconstruction precision

Похибкою вимірювання положення треку будемо називати різницю між дійсним положенням треку  $r_{track}$  and reconstructed  $r_{rec}$ . Дану точку відобразим на графіку з відхиленням по осі Y та дійсним положенням треку по осі X. Для більшої наглядності ситуації з розподілом точок на графіку зобразимо цю ж інформацію у вигляді діаграми густини точок а також у вигляді структурної діаграми для оцінки абсолютної похибки.

Варто зазначити, калібровочна крива не проходить через точку  $(0;0)$ , то ж значення часу дрейфу ліворуч від кривої будемо співставляти центральний трек (такий, що проходить через центр дрейфової трубки  $r = 0$ ). Схоже правило застосовується для сигналів з часом дрейфу більшим за діапазон охоплений калібровочною кривою - таким сигналам  $r_{reconstructed}$  присвоюється значення  $r_{tube} = 4.9mm$ .

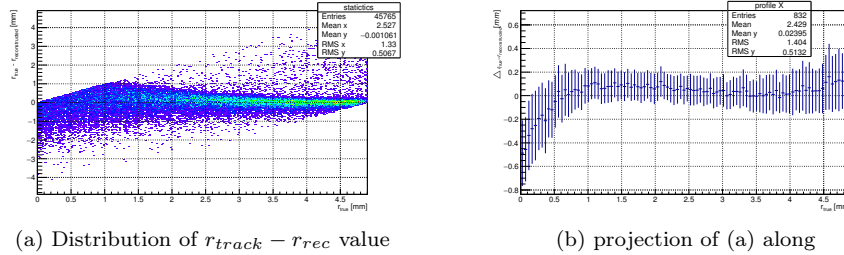


Рис. 17: Distribution of Розподіл різниці між дійсним і реконструйованим положенням треку в трубці  $\Delta_{r_{track}-r_{rec}}$  від 49500 подій. Структурна діаграма розподілу точок у випадку строго центрального положення дроту дрейфової трубки

Як видно з простого аналізу діаграми Рис. 17a 17b точність реконструкції позиції треків лежить в діапазоні  $(0.1 \dots 0.2)mm$ .

### 6.5 Випадок зміщеного дроту

Знаходження калібровочної кривої, якщо її так можна назвати, для випадку зміщеного дроту дещо відрізняється від описаного вище центрального випадку. Це пов'язано з несиметричністю розподілу "час дрейфу - положення треку" Рис. 12b. Тож необхідно знайти не одну, а дві калібровочні криві, причому необхідно розділення даних (на гілки більшу-меншу) що неможливо без попередньої оцінки величини зміщення дроту від центрального положення.

Як видно з Рис 12b фігура розподілу змінилася не значно, а лише зсунулася на сталі значення, рівне зміщенню дроту.

Використаємо цю хитрість для розбиття даних на дві частини - дві гілки в RT розподілі. Від так ми можемо для кожної гілки знайти свою власну калібровочну криву.

## 329 6.6 Порівняння розподілів для центрального та зміще- 330 ного позицій дроту в трубці

331 Наведемо порівняння гістограм для центрального та зміщеного позицій  
332 дроту для вибірки треків в околі дроту та на відстані 2 мм від нього.

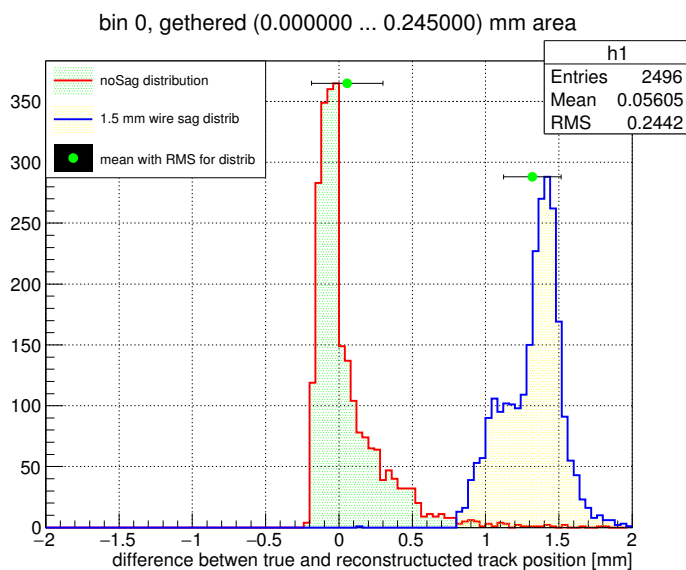


Рис. 18: Порівняння розподілу реконструкції позицій треків для центрального положення дроту та випадку зміщення дроту дрейфової трубки на  $1.5\text{mm}$  від центрального положення для треків які проходять близько до центру трубки

333 Цілком логічно припускати, що електроніка реєструватиме час дрейфу  
334 відмінний від триманого нами від симуляцій описаних вище. Тож необх-  
335 дним буде врахувати внесок від електроніки. Ситуація ускладнюється тим  
336 що окрім форми вхідного сигналу потрібно знати ще й амплітуду сигна-  
337 лу(сумарний заряд зібраний з треку з урахуванням підсилення).

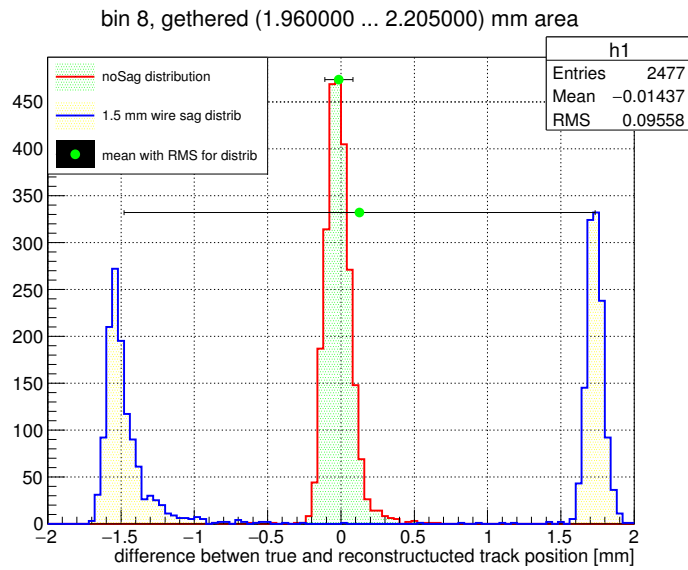


Рис. 19: Порівняння розподілу реконструкції позицій треків для центрального положення дроту та випадку зміщення дроту дрейфової трубки на  $1.5\text{mm}$  від центрального положення для треків які проходять дотично до кола радіусом  $2\text{mm}$  коцентричного з трубкою

## 338 Література

339 [1] <http://garfield.web.cern.ch/garfield>

340 [2] thesis Kozlinskiy.pdf